Dirty Paper Coding for Gaussian Cognitive Z-Interference Channel: Performance Results

Zouhair Al-qudah and Dinesh Rajan, *Senior Member, IEEE*

***Abstract*—In this paper, we present a practical application of dirty paper coding (DPC) for the Gaussian cognitive Z-interference channel. A two stage transmission scheme is proposed in which the cognitive transmitter first obtains the interference signal from the primary transmitter and then uses DPC to improve the performance of the cognitive link. Numerical results show that causal knowledge of the interference provides more than 3 dB improvement in performance in certain scenarios over a scheme that does not use interference cancellation. Results are also shown when the cognitive transmitter operates in both half-duplex and full-duplex modes.**

***Index Terms*—Dirty paper coding, cognitive transmitter, channel coding, decoding, Z-interference channel.**

I. Introduction

THE recent growth in wireless technologies has been nothing short of phenomenal. However, there is a rapid recognition that the performance of future wireless networks are likely to be limited by interference. Consequently, interference management techniques such as smart scheduling, interference cancellation, interference alignment, and dirty paper coding are receiving significant attention. These interference management techniques include those that are employed only at the transmitter, only at the receiver, or both. In parallel, the improved reconfigurability of hardware platforms is making the dream of a software defined radio based cognitive network closer to reality. The focus of this paper is to study a practical interference cancellation method at the transmitter of a cognitive interference network.

Interference cancellation at the transmitter, was originally studied by Gelfand and Pinsker in which they proved that the capacity, C, of a discrete memoryless channel with input, X, output Y, side information S available to the transmitter but not to the receiver and is given by [1], [2]

$$C = \max_{p(u,x|s)} \{I(U;Y) - I(U;S)\} \tag{1}$$

where U is an auxiliary random variable and I represents the mutual information. Subsequently, in his path breaking work, Costa [3] applied the previous capacity formula to the additive Gaussian noise channel to prove that an interference free channel capacity can be achieved. In particular, he considers the problem of communicating over a channel modeled as

$$Y = X + S + Z \tag{2}$$

where Y represents the channel output, X represents the channel input and finally S and Z are the additive interference signal and the additive white Gaussian noise (AWGN) signal, respectively. In his work, Costa made two main assumptions to achieve the channel capacity, the interference is available non-causally at the transmitter only and the random variable U is designed to be $U = X + \beta S$ where β is the power inflation factor. This power inflation factor is a critical factor that determines the appropriate scaling of the interference signal to use in constructing the DPC code. It has been shown that for such a model, the optimal $\beta = \frac{P_X}{P_X+P_Z}$, where P_X and P_Z are the power variance of both the desired signal X and the additive noise signal Z, respectively.

In addition to this DPC scheme, several other alternatives have also emerged to cancel the effect of the interference including, zero-forcing [4], [5], and zero forcing dirty paper coding (ZF-DPC)[6]. Compared to DPC, ZF-DPC is a lower complexity but suboptimal interference cancellation technique [7], [8]. In this paper, we also briefly compare our results with linear ZF interference cancellation and find that the performance of the later is inferior to the proposed scheme. The Interference cancellation techniques at the transmitter may also require cooperation between the senders and/or receivers to avoid interference between users sharing the same spectrum. In the classical two-user Gaussian interference channel, transmitters cooperation is studied in several settings including in a unidirectional noncausal cooperation link [9], [10], in a bidirectional noiseless link [11], or in noisy bidirectional channels [12]. These scenarios are also studied in the one sided interference channel, which is known as Z-Interference channel (ZIC). For instance, the authors in [13] studied the Gaussian cognitive (ZIC) shown in Fig. 1 and computed the achievable rates between nodes C and D when node C has partial, causal, and noisy information about the signal transmitted by node A.

Simultaneous to these theoretical developments, practical DPC techniques have also been proposed for the SISO additive Gaussian channel [14], [15], the MIMO broadcast channel [16], and for cognitive radio channels [17]. These DPC techniques typically use a combination of a vector quantizer and a capacity-approaching channel code like low density parity check (LDPC) code [14], [18], [19]. LDPC has been widely adopted in many wireless standards including Digital Video Broadcasting - Satellite - Second Generation (DVB-S2),

Manuscript received November 26, 2012; revised May 24 and September 12, 2013; accepted September 13, 2013. The associate editor coordinating the review of this paper and approving it for publication was M. Ardakani.

Z. Al-qudah is with the Department of Communication Engineering, Al-Hussein Bin Talal University at Ma'an, Jordan (e-mail: qudahzuhair@gmail.com).

D. Rajan is Professor of Electrical Engineering at Southern Methodist University (e-mail: rajand@lyle.smu.edu).

Digital Object Identifier 10.1109/TWC.2013.102313.121869

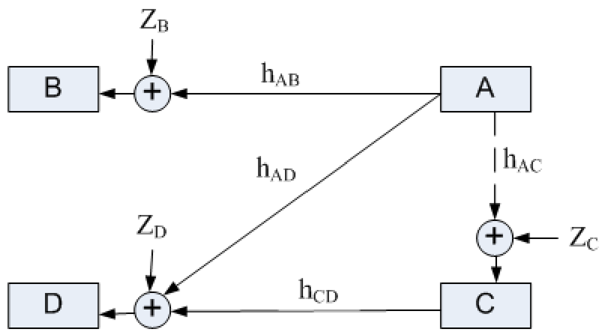

Fig. 1. Gaussian Z-Interference Channel with Cognition from node A to node C.

WiMAX (IEEE 802.16e) and WiFi (IEEE 802.11n).

In [13], the achievable rates is derived based on traditional information theoretic random codes with infinite length. Thus, the rate obtained provides only the theoretical scenario but not directly applicable to the code design of real system. However, in practical communication scenario, the codeword length must be finite. In this paper, we develop a practical and causal transmission strategy to improve the rate between nodes C and D. Specifically, we propose a two-phase transmission scheme in which we initially estimate the interference signal and then employ DPC to mitigate the effect of this interference. In the proposed system, the cognitive transmitter (node C) listens to the signal of node A for a portion of its codeword and then decodes the available portion. In this regard, the node A's portion that node C has to listen is bounded. Then, node C estimates the remaining fraction of the node A's signal. Based on this estimate, node C employs DPC to improve the rate of communication on link $C-D$. In addition, the power inflation factor is derived in the case that a noisy causal interference signal is available at the cognitive transmitter. In this derivation, we account for the value of having the gains of both the channel from the interference source (node A) to the receiver and from the cognitive transmitter (node C) to the receiver at the cognitive transmitter. In particular, we convert the cognitive radio channel into its equivalent modulo lattice additive noise (MLAN) channel by using lattice based DPC described in [20]. In this regard, lattice codes is a capacity achieving codes having a structure with low complexity [21], [20]. For instance, lattice codes is used to achieve the AWGN channel capacity [21], and the capacity of channels with interference available non-causally at the transmitter [20], [18].

Our results indicate that even when the received power at node D of the interference signal from node A is as high as the signal power from node C, the proposed causal DPC scheme provides significant reduction in the bit-error-rate (BER) over a scheme that does not employ interference cancellation. For comparison, the performance of a noncausal DPC scheme is also provided and indicates that the performance of the proposed causal scheme depends on the SNR of link $A-C$. Clearly, the reliability of estimation the interference signal at node C plays an important role in determining the overall system performance. We present results when node C operates in both half-duplex and full duplex modes. In half-duplex mode, the fraction of time that node C listens to the signal from node A determines the reliability of estimating the interference signal at node C and consequently the performance of the cognitive radio link. In full-duplex mode, node C can simultaneously receive the signal from node A and transmit a signal to node D. In this case, we demonstrate the benefits of updating the estimate at node C of the interference signal and using these for DPC. Clearly, there is a trade-off between the computations involved in the update and the resulting performance.

The remainder of this paper is organized as follows. In Section II the system model as well as the DPC scheme are presented. DPC for the causal system is described in Section III. Numerical results are given in Section IV followed by brief conclusions in Section V.

II. System Model and DPC System Overview

In this section, we first introduce the cognitive Z-interference channel model. Then, we review the basics of a practical DPC for a point-to-point system with known noncausal interference at the transmitter.

A. System Model

The cognitive ZIC as shown in Fig. 1 is considered. It contains two transmitters and two receivers where the primary transmitter (node A) communicates with its intended receiver (node B) and the secondary transmitter (node C) communicates with its receiver (node D). We focus on the case when node C is closer to node A than node B so that it can decode node A's message based on listening to a portion of its codeword. Subsequently, node C starts transmission to its intended receiver employing DPC as described in the sequel. Further, for the majority of the paper, we assume that node D can not reliably decode node A's signal, *i.e.*, interference cancellation is not possible at the receiver. For instance, this model might occur in a certain system where node A is a base station and node B is a mobile user at the cell edge. Nodes C and D could represent additional users in the system that wish to communicate directly with each other. We briefly address the case that node D can also decode the signal from node A and perform an interference cancellation.

In a non-causal DPC scheme the interference signal from the primary source is assumed to be available at the cognitive transmitter before both the transmitters start sending their messages. On the contrary, in the causal case, the cognitive sender does not have knowledge of the primary user's signal. The cognitive transmitter has to listen to the primary user's transmission for a portion of time in order to estimate the interference signal prior to commencing its own transmission. The focus of this paper is on the causal DPC scheme. However, for comparison the BER of a non-causal DPC scheme is also shown in the numerical results.

B. Dirty Paper Coding Scheme

The transmitter contains two main blocks: i) an LDPC channel encoder that provide temporal diversity gain, and ii) a vector quantizer (VQ) [22], [23] to compensate for the known interference. Consider the transmission of a m bit information sequence $u = (u_1, u_2, \ldots, u_m)$. This sequence is first encoded using a rate m/n LDPC encoder to generate output $c = (c_1, c_2, ..., c_n)$ of length n and then modulated using a M-QAM constellation as shown in Fig. 3(a). In parallel to these operations, the interference signal x_A is first multiplied by the power inflation factor (β) and then fed to a two dimensional modulo lattice operation to form the modified interference signal $x_A^{'}$. Subsequently, the mapped data bits from the LDPC encoder and $x_A^{'}$ are passed to the VQ to select the stream of symbols that minimize the distance between them using the Viterbi algorithm. Finally, the difference between the quantized value q_i and $x_{Ai}^{'}$ is transmitted. Note on notation: x_A is used to represent the available noncausal interference whereas $\tilde{x}_A$ is used to represent the estimated causal interference.

The primary objective of the dirty paper coding scheme is to generate a coded sequence that is *close* to the interference signal. This objective is achieved by generating for each codeword of the LDPC code, a group of equivalent codewords that are distributed over the entire signal space using a procedure that is similar to [14], [15], [18]. In this process, the codeword sequence, from this equivalent group of codewords, that is closest to the interference signal is selected and will by design have a smaller distance than between the original LDPC codeword and the modified interfering signal $x_A^{'}$. In particular, each symbol d_i from the M-QAM constellation works as an offset for the N-QAM constellation. Now, for each shifted symbol from the N-QAM, the set of modulo equivalent points is formed. After that, the Viterbi algorithm is employed to select the stream of symbols that minimize the Euclidean distance with the modified interfering signal $x_A^{'}$.

Fig. 2 shows the constellations for both the data mapper (M-QAM) and the one for the VQ (N-QAM). The distance between adjacent constellation points in both the constellations are designed such that the modulo equivalent points do not interfere. In addition, the relation between the constellation size of the VQ and its coding rate can be easily given as [21]

$$R_{VQ} = \log_2(N_r) = \log_2\left(\frac{1}{N}\right) \tag{3}$$

where N_r is the nesting ratio of the nested lattice code and N is the constellation size of the VQ. Now, to ensure that the receiver can successfully decode from among these equivalent points, we use a convolutional code $(d_i, x_{Ai}^{'}, q_i, K)$ to ensure that the selected sequence of symbols is a valid codeword. Here, d_i and $x_{Ai}^{'}$ are the two inputs to the VQ from the M-QAM constellation and the modified interference signal, respectively. Moreover, q_i is the quantized output and K is the constraint length of the VQ's convolutional code. In effect, the symbols are being processed using a VQ that finds the sequence that is closest to the *modified* interference signal. The sequence of outputs of the VQ form a valid codeword of the underlying convolutional code. An alternate view is to think of the selected sequence as a valid codeword both for the LDPC code and for the convolutional code.

The received signal is first multiplied by the power inflation factor β and then processed by a non-linear modulo operation

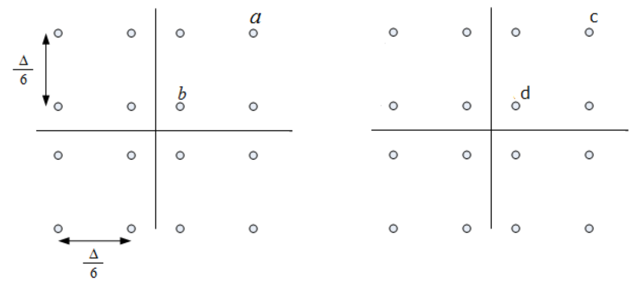

(a) N-QAM of the vector quantizer (b) M-QAM of the mapper

Fig. 2. The constellation for both the mapper and the vector quantizer. The dimensions are $a = (\frac{\Delta}{4}, \frac{\Delta}{4})$,$b = (\frac{\Delta}{12}, \frac{\Delta}{12})$, $c = (\frac{\Delta}{16}, \frac{\Delta}{16})$, and $d = (\frac{\Delta}{48}, \frac{\Delta}{48})$.

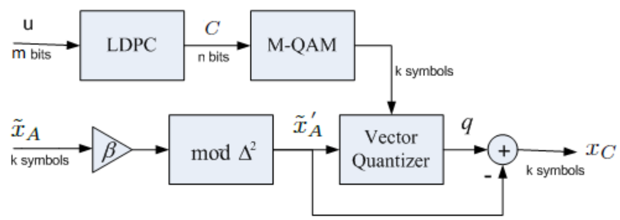

(a) Transmitter section (Node C)

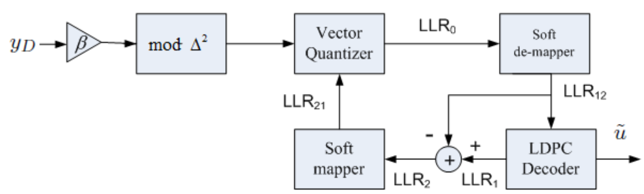

(b) Receiver section (Node D)

Fig. 3. Dirty paper Coding Transceiver System [14], [15].

mod Δ^2. Thus, by both exploiting the availability of the interference at the transmitter and the structure of the transmitter as well as the receiver ensures that an interference free received signal is obtained. Finally these signals are fed to an iterative decoder to obtain the transmitted data sequence. In the interest of space, we refer the reader to [14], [24], [25] for additional details.

As noted before, the signal q is a codeword both of the convolutional code as well as the LDPC code. The iterative decoding works as follows. First we use the BCJR based MAP decoder for the convolutional code (BCJR-VQ) [14], [15] that computes the a-posteriori information of the symbol sequence $q_i^{'}$ where $i \in (1, ..., k)$ based on the received signal and the a priori information provided by the channel.

Then, the soft de-mapper computes the extrinsic information that are passed to the LDPC decoder as [26], [24]

$$LLR_{12}(d_i^j) = \ln \frac{\sum_{d_i^j=1} \; e^{LLR_0(d_i)}}{\sum_{d_i^j=0} \; e^{LLR_0(d_i)}} \tag{4}$$

where $j \in [1, N]$ represents the bit position in symbol i. In other words, the a priori probabilities of a bit at the input of the LDPC decoder is computed over all symbol values which contains the related bit values.

The LDPC decoder employs the sum product algorithm

(SPA) which gives a posteriori probabilities about the LDPC coded bits. In the next iteration, this a posterior information is passed as the new a priori information to the BCJR-VQ decoder. The iteration stops after the desired stopping criterion is met, and the LDPC decoder outputs the decoded codeword and the a posteriori probabilities of the data bits is computed [26], [24] by the soft-mapper as

$$LLR_{21}(d_i = d_i^1 ... d_i^N) = \prod_{j=1}^{N} \frac{e^{d_i^j LLR_2(d_i^j)}}{1 + e^{LLR_2(d_i^j)}} \tag{5}$$

where $LLR_2 = LLR_1 - LLR_{12}$, and LLR_1 is extrinsic information provided by the SPA algorithm. In other words, the a priori value of a symbol at the input of the VQ decoder over all possible bit combinations is calculated. Essentially, the soft mapper and de-mapper relate the bit a priori probabilities with the symbol a priori probabilities.

III. DPC For Causal Systems

In this section, a two phase encoding technique is proposed that first estimates the interference signal and then mitigates its effect by employing DPC at the cognitive transmitter. Moreover, we consider the cognitive transmitter operating in both half-duplex and full-duplex nodes.

First, we consider the case that node C uses half-duplex transmission. Let node A transmit using a systematic LDPC code with a generator matrix of size $M_1 \times N_1$ and code rate $r_A = \frac{M_1}{N_1}$. In this formulation, M_1 represents the data-word length and N_1 is the LDPC codeword length. Furthermore, we assume that node C has knowledge of node A's code book but not the exact codeword being transmitted. Node C listens to the first εN_1 bits of node A's codeword, where ε is a fraction that will be computed later. Clearly, for node C to be able to successfully decode node A's signal, ε has to be greater than $\frac{M_1}{N_1}$. Further, node C is able to decode node A's signal and then get the first M_1 bits only if [27], [28]

$$r_A R_m \leq \varepsilon \log_2 \left(1 + |h_{AC}|^2 \frac{P_A}{P_{z_C}} \right) \tag{6}$$

where R_m is the modulation rate in bits e.g. $R_m = 2$ bits for 4-QAM. In addition, h_{AC} is the channel gain from the primary user to the secondary transmitter, P_A is the transmit signal power from the primary user and finally P_{z_C} is the noise variance at the secondary transmitter.

The received signal y_C at node C is given by,

$$y_C = h_{AC} x_A + z_C \tag{7}$$

where x_A is the signal transmitted by node A, and z_C is the AWGN at node C. Subsequently, node C decodes the received signal using the first εN_1 bits of y_C and then estimates the remaining $(1 - \varepsilon)N_1$ bits of $\tilde{x}_A$. Node C then uses these estimated $(1 - \varepsilon)N_1$ bits as the available interference, and employs a DPC to adapt its signal for transmission. Specifically, node C uses LDPC as a channel code and a VQ to deal with the available causal interference. In particular, the LDPC code has a generator matrix of size $M \times N$, where $M = (1-\varepsilon)M_1$ and N is selected based on the required error protection over the cognitive link, i.e., the value of N has to be increased for a lower BER. The specific structure of the DPC system used at node C is shown in Fig. 3(a).

The received signal, y_D, at node D is given by

$$y_D = h_{CD} x_C + h_{AD} x_A + z_D \tag{8}$$

where x_C is the transmitted signal by node C, x_A is the interference signal from node A, and z_D is the AWGN. In addition, h_{CD} is the channel gain of the cognitive radio link, and h_{AD} is the channel gain from the primary transmitter to the cognitive receiver. Furthermore, these channel gains are assumed to be known to the cognitive transmitter [29], [16]. The received signal is first multiplied by the power inflation factor (β) and then subjected to a two dimensional modulo operation. The output of this modulo function is fed to an iterative decoder as depicted in Fig. 3(b). Since the estimated interference signal is a noisy one, the power inflation factor $\beta = P_C/(P_C + P_{z_D})$ derived in [18], [14] is no longer optimal. Thus, the optimal value of the power inflation factor is computed as

$$\beta = \frac{|h_{CD}|^2 P_C}{|h_{CD}|^2 P_C + \frac{|h_{AD}|^2}{|h_{AC}|^2} P_{z_C} + P_{z_D}} \tag{9}$$

Proof: See the Appendix.

Further, the data rate over the cognitive link is given as [13]

$$R_{CD} \leq (1 - \varepsilon) \log_2 \left(1 + \frac{|h_{CD}|^2 P_C}{P_{z_D} + \mu_t(m) |h_{AD}|^2 P_A} \right) \tag{10}$$

where m, $M_1 \leq m < N_1$ is the number of bits that node C has to listen in order to estimate the remaining bits $(N_1 - m)$. In addition, $\mu_t(m) = \frac{N_1'(m)}{N_1'(m) + P_A}$, $N_1'(m) = 2P_A P_{e,C}(m)$, and $P_{e,C}(m)$ is the error probability of estimating the interference signal at the secondary transmitter in phase 1. Moreover, the relationship between m and $P_{e,C}$ will be numerically studied in the next section.

Together (6) and (10) bound the value of ε as shown in (11). In particular, a lower bound can be calculated from (6) whereas the upper bound can be simply found from (10). In this derivation, for a given value of $r_A R_m$, the lower bound is explained as follows

1) In the low SNR_{AC} regime of the link $A - C$, node C has to listen to more than M_1 bits in order to efficiently estimate the data bits M_1. In this case, the value of ε should be selected as $\varepsilon \geq \frac{r_A R_m}{\log_2 \left(1 + |h_{AC}|^2 \frac{P_A}{P_{z_C}} \right)}$. In other words, node C has to listen to node A for more portion of the data to efficiently estimate the interference signal from node A.
2) In the high SNR_{AC} regime, it is satisfactory for node C to listen only to the first M_1 bits. In this case, $\varepsilon \geq r_A$ should be selected. Thus, listening only to the data bits are sufficient to generate the interference signal.

Remarks-1:

- For a given constellation size at node C, the value of ε is inversely proportional to the amount of data that node C can transmit.
- The value of $\varepsilon = 0$ refers to the case of transmission over the ZIC without employing DPC at the secondary transmitter.

$$\max\left(r_A\ ,\ \frac{r_A R_m}{\log_2\left(1+|h_{AC}|^2\frac{P_A}{P_{z_C}}\right)}\right)\le\varepsilon\le 1-\frac{R_{CD}}{\log_2\left(1+\frac{|h_{CD}|^2P_C}{P_{z_D}+\mu_t(m)|h_{AD}|^2P_A}\right)} \tag{11}$$

- The case of $\varepsilon = 1$ means that node C does not transmit any data to its destination.

If node C is a full duplex node, then it listens only to the first $r_A N_1$ bits of node A and then begins its transmission. In this case, ε is equal to r_A. However, node C continues to receive node A's signal and periodically updates its estimate of the interference signal. For each update, node C modifies its transmitted signal to account for the *improved* estimate of the interference. Note that as the frequency of updates increases, the computational complexity also increases. The performance improvements for various rates of updating the interference is shown in the following section.

IV. Results and Discussions

In this section, we present numerical results of the proposed technique. Node A uses a rate $1/2$ LDPC with a generator matrix of size $(840, 1680)$ having 3 ones per row. Also node C uses a rate $1/2$ LDPC with a generator matrix of size $(M, 2M)$ having 3 ones per row; the value of M depends on the value of ϵ and will be specified later. Unless otherwise specified, the VQ employs the Viterbi algorithm with code rate $1/2$ at node C and the BCJR algorithm at node D. This convolutional code (CC) has constraint length $K = 7$ and generator polynomial $[133\ 171]$. These values of the generator polynomials give the best performance for the given constraint length [30]. For simplicity, we assume that both node A and node C transmit using the same constellation size (4-QAM). Our results have been obtained for 3 iterative decoding iterations and 150 iterations for the LDPC-decoder [14].

A. Performance over the cognitive Z-Interference Channel.

Recall that the primary sender in an interference channel can transmit its signal using the Han-Kobayashi scheme in which both a common message and a private message are sent.

As the name suggests, the private message can be typically only be decoded by the primary destination, and in this case, also by the cognitive transmitter. However, under certain circumstances, the common message can be decoded at both receivers. In particular, Fig. 4 shows two regions in which the interference cancellation can be done at either the cognitive transmitter or the cognitive receiver. The first region is related to the case of weak channel gain, h_{AD}, where interference cancellation at the transmitter using DPC can outperform interference cancellation at the receiver. In the second region, which is related to the case of very strong interference, the cognitive destination can first decode the common message from the primary user and then cancel out its effect. Afterwards, the cognitive receiver can decode the intended signal from the cognitive transmitter. The major focus of this paper, is to study interference cancellation in the first region, where DPC is employed at the cognitive transmitter. In practical systems, a combination of both methods could be employed.

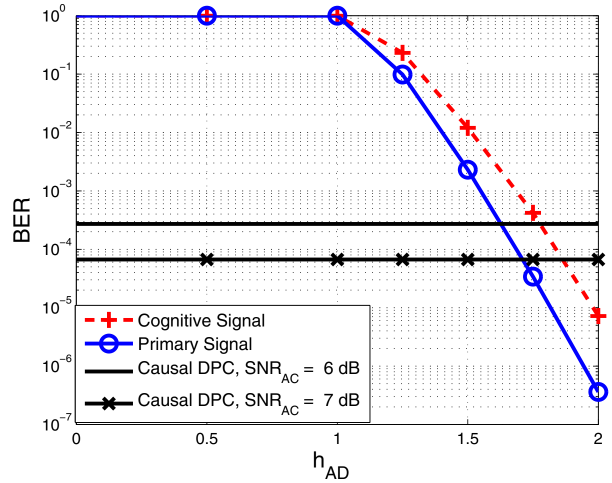

Fig. 4. Different interference cancellation techniques over the cognitive link. Further, we fix $SNR_{CD} = 5dB$.

For instance, in Fig. 4, when the $SNR_{AC} = 6$dB, for values of h_{AD} that are greater than 1.8, interference cancellation at the receiver of the common message can provide lower BER than DPC. For values of h_{AD} that are smaller than 1.8, DPC at node C offers lower BER than interference cancellation at node D. This threshold of 1.8 increases as SNR_{AC} increases.

B. Performance over the cognitive Link.

Now, we numerically study the bounds on ε. For simplicity, we assume that the channel gains across all users are normalized i.e., all the channel gains are equal to 1. Moreover, we select the SNR_{AC} of the link $A - C$ to be ≥ 5 dB so that the lower bound in (11) is reduced to $\varepsilon \ge \max(r_A, \frac{1}{\log_2(1+\sqrt{10})}) = 1/2$ for the case that $r_A = 1/2$.

Fig. 5 addresses the accuracy of estimating the interference signal causally at the cognitive transmitter. In particular, this figure shows the bit error rate (BER) for both decoding the data bits of node A and also the BER of the estimated interference bits at the cognitive transmitter. As expected, the BER's of estimating the interference signal decreases as ε increases. Further, it can be seen that for a given SNR, the BER of estimating the $(1-\varepsilon)N_1$ bits is approximately 1 to 2 orders of magnitude higher than the BER of the first εN_1 bits. Specifically, this gap in performance is due to the non-sparsity of the LDPC generator matrix G, *i.e.*, the occurrence of a single data bit error can leads to multiple errors (equal to the number of 1's in the corresponding row of the generator matrix) in the estimates of the coded bits. Moreover, this error in the reliability of obtaining the interference signal dominates the error rate of the cognitive radio link as will be evident from the subsequent results.

Remarks-2: If node A transmits using another modulation scheme such as 16-QAM, then the reliability of estimating

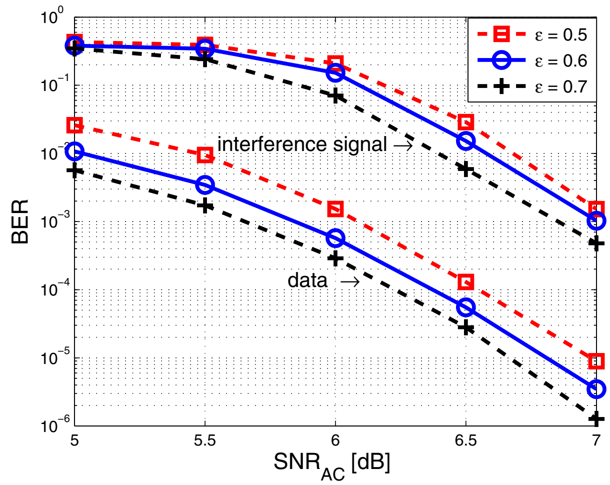

Fig. 5. BER for (i) estimating the data bits of node A at node C, and (ii) generating the interference signal that affects the cognitive radio link. We use εN_1 to estimate the data word, M_1 bits. Then these M_1 bits are used to generate the redundant bits, $N_1 - M_1$. Thus, the interference signal, $(1-\varepsilon)N_1$ bits, is generated.

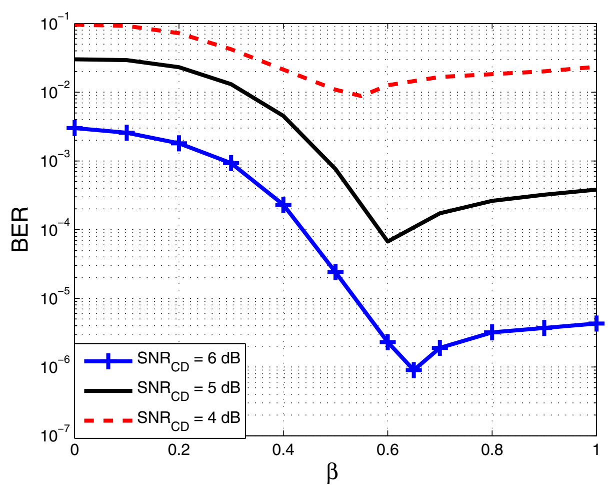

Fig. 6. BER over the cognitive link in which a various values of β is used in the case that the cognitive transmitter is working in the half-duplex mode with $\varepsilon = 0.5$.

the interference signal, from the primary user, reduces. Thus, node C would need to listen to a larger fraction of node A's transmission than in the case of 4-QAM.

C. Optimal β versus non-optimal β

To illustrate the benefits of using the optimal β, we plot in Fig. 6 the BER of link C-D for various values of β. This figure clearly shows that significant reductions in BER are possible by selecting the optimal value of β. This optimal value of β given by (9) matches numerically with the dips in the figure for various values of SNR_{CD}. The increase in BER with a non-optimal choice of β is a consequence of the interference not being completely cancelled.

In the next two subsections, we discuss the performance over the cognitive link when node C is in either half-duplex or full-duplex mode.

D. Half Duplex: Numerical Examples and Discussions

Now, we discuss the performance of the cognitive radio link for the case that node C operates in half-duplex mode. Further, we show how the reliability of estimating the interference signal can dramatically improve/degrade the system performance. Fig. 7 shows the BER for six different cases. Specifically, in the first three cases, the following $(840, 1680)$ regular LDPC code is used. First, for comparison, we show the BER for a system in which a noisy non-causal interference is available at node C and the cognitive channel is corrupted by both AWGN and interference. Second, we show the performance of a system without any interference cancellation. In particular, these two results act as the upper bound and lower bound on the BER over the cognitive link in the case that a $1/2$ LDPC code is used at the cognitive transmitter. Third, we show the performance of the channel from node C to node D in the presence of AWGN only, i.e., interference free link. Fourth, we also show the performance of the proposed causal DPC technique. We fix the SNR_{AC} of the channel from node A to node C as $SNR_{AC} = 7dB$ such that node C can acquire the interference signal. Clearly, the value of ε plays an important role in the reliability of estimating the interference signal at node C. In this case, the probability of decoding error in estimating node A's signal at node C varies from $2 * 10^{-3}$ for $\varepsilon = 0.5$ to 10^{-3} for $\varepsilon = 0.6$. The following regular LDPC codes $(420, 840)$ and $(336, 672)$ are used by node C for $\varepsilon = 0.5$ and 0.6 respectively. As shown in the figure, both the reliability of estimating the interference signal at node C as well as the value of ε determines the performance of the cognitive radio link. In addition, as the SNR_{AC} increases, the gap to the non-causal case reduces. Fifth, to compare in performance and throughput, we transmit the same number of useful data over the secondary link without employing DPC but using a lower LDPC code rate. Remember that in the case of $\varepsilon = 0.5$, the following $1/2$ LDPC code with a generator matrix of size $(420, 840)$ is used. Instead, a $1/4$ LDPC code with generator matrix $(420, 1680)$ is employed. This again shows the importance of using our proposed technique over the cognitive link. Finally, we compare the performance of the proposed method a with zero-forcing system[4], [5], which was originally proposed for bi-directional cognitive interference channel. In this case, the cognitive transmitter allocates a part of its power to cancel the effect of the interference from the primary user. The amount of this power allocation depends on both h_{AD} and P_A. For instance, for $h_{AD} = \frac{1}{\sqrt{2}}$, and $P_A = 1$, the results in Fig.7 is obtained. Clearly, the performance of the zero-forcing method is inferior to that of the proposed DPC method. However, it should be noted that the complexity of the linear zero-forcing method is also much smaller. For larger values of h_{AD} the performance of the zero-forcing method would deteriorate even more as compared to the DPC scheme.

Remarks-3:

- We note that the curve with $1/4$ LDPC code is obtained in the case that $P_A = P_{Z_D}$. However, the BER over the cognitive link will increase further for values of *interference signal power* P_A that is larger than P_{Z_D}. In contrast, in the technique we use, the reliability over

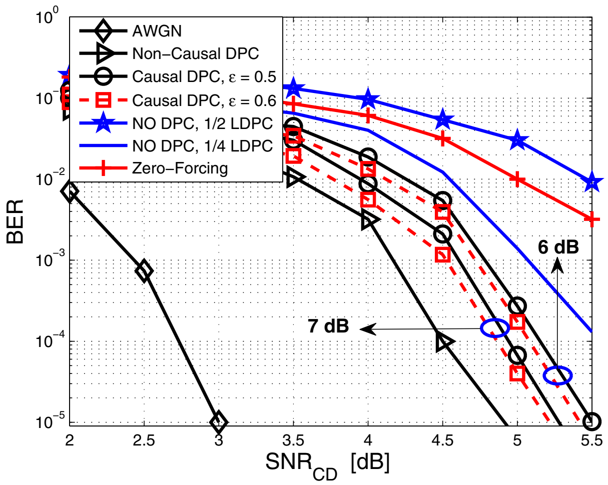

Fig. 7. BER comparison between system with non-causal interference and causal interference for different values of ε in the case that node C is in half-duplex mode. 6 dB and 7 dB are referred to different cases of the channel quality of the link $A-C$.

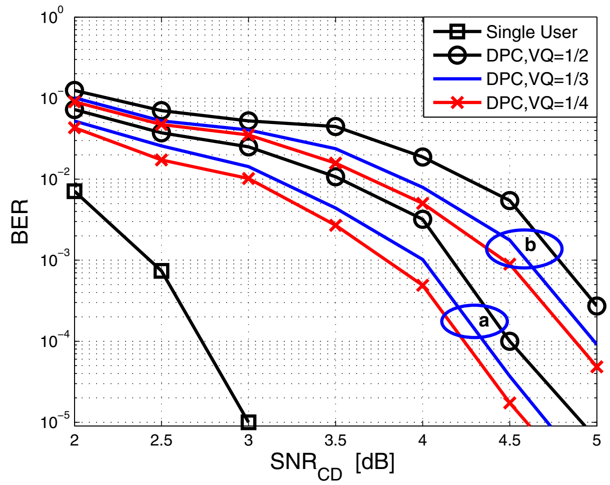

Fig. 8. System performance with different VQ's code rate: (a) Non-causal interference (b) Causal interference with $\varepsilon = 0.5$.

TABLE I
CODES AND THEIR GENERATOR POLYNOMIALS [30].

Code rate	Generator Polynomial
1/2	(133 171)
1/3	(133 165 171)
1/4	(117 127 155 171)

the cognitive link is mainly affected by the reliability of estimating the interference signal but not the power of the interference signal.

- The gap between the noncausal DPC and the interference free AWGN is due to mainly the quantization process at both the transmitter and receiver.
- The gap between the noncausal DPC and causal DPC is due to two reasons. The primary reason is the noisy estimate of the interference signal at the cognitive transmitter. A secondary reason is the variation in the LDPC code lengths that are used, *i.e.*, a $(840, 1680)$ LDPC is used in the noncausal case whereas a $(420, 840)$ is used in the causal scenario. Recall that for a given code rate, increasing the code length can reduce the BER.
- In the case that node C transmit using 16-QAM, then the constellation in Fig. 2(b), is used and can increase the BER at node D.

Next, we discuss two important techniques that can be used to reduce the BER over the cognitive link: i) using a more powerful VQ, and ii) employing full-duplex transmission instead of half-duplex transmission at node C.

There are many different techniques in the former category, including increasing the constraint length of the VQ or using a VQ with different code rate. It is reported in [31], [14] that increasing the constraint length of the VQ can improve the system performance approximately 0.2 dB. Fig. 8 shows how the BER of the non-causal as well as causal DPC can be reduced when using a vector quantization with variable coding rates. Specifically, different CC's are considered, all with constraint length $K = 7$, but characterized by different code rates and generator polynomials as shown in Table. I. Clearly, using a VQ with smaller code rate improves the BER, at the cost of increasing the computational complexity of the system.

Further, we illustrate the trade-off between data rate and reliability over the cognitive link based on the reliability of estimating the interference signal at node C. For a given SNR for both links, the results are shown in Fig. 9. Clearly, as the data rate increases so does the BER. Further, improving the reliability of estimating the interference signal can significantly reduce the BER. Moreover, we note that, for a given constellation size at the cognitive transmitter, the data rate is inversely proportional to ε. This figure also shows a comparison between systems that employ DPC and those do not. Specifically, for data rates 0.25 and 0.5, it is clear that the proposed technique performs better than systems that do not employ DPC. We remark that the rates 0.25 and 0.5 are related to the previously used LDPC codes over the secondary link without employing DPC and with coding rate $1/4$ and $1/2$, respectively.

E. Full Duplex: Numerical Example and Discussion

In this subsection, results for the case that node C is a full-duplex mode are presented. We initially let node C listen only to the data bits of node A, *i.e.*, $\varepsilon = 0.5$ and then commence its transmission after decoding the information about node A. Recall that in full duplex mode, ε is designed to be equal to node A's code rate. Further, after decoding node A's data, node C starts transmitting to its destination node D and also in the meantime updating its estimates regarding the interference signal from node A. Let node C update its estimate of node A's signal every subsequent 5%, *i.e.*, for $\varepsilon = 0.55, 0.6, \cdots, 0.95$. This update ensures that the interference signal can be obtained in a progressively more reliable manner. In this case, every frame of node C is divided into blocks equals to the number of updates plus one. Now, every block of data is processed and transmitted based on the

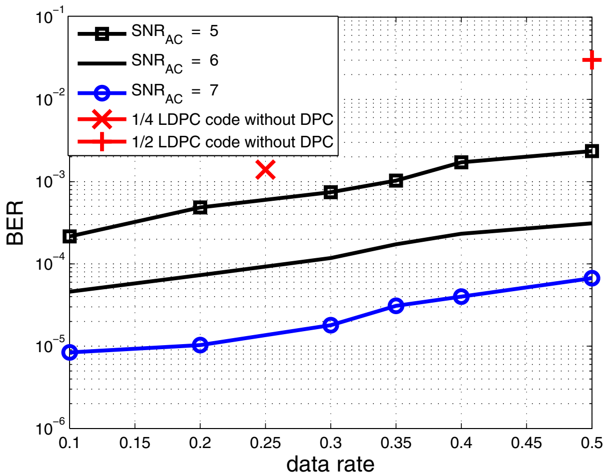

Fig. 9. Tradeoff between data rate and Reliability for $SNR_{CD} = 5$ dB. This figure also compares data rates between system using cognitive causal DPC and that does not employ DPC.

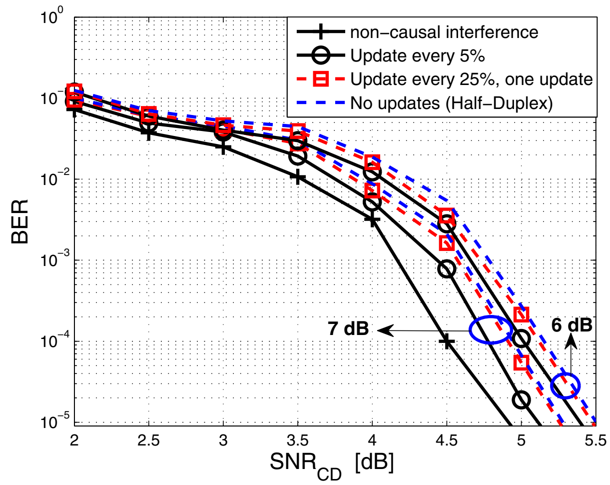

Fig. 10. Performance of the channel between node C and node D for Full-Duplex transmission and different values of updates. The curve without updates is the same as half-duplex with $\varepsilon = 0.5$. In addition, 6 dB, and 7 dB are the signal to noise of the link $A - C$.

available estimate of the interference signal. At the receiver, each block is multiplied by the power inflation factor (β) and then fed to the non-linear modulo lattice filter. Specifically, all consecutive blocks, that are related to one frame, are serially grouped and fed to the iterative decoding which is depicted in Fig. 3(b) [32]. We note that the error in such a system is mainly due to using $\varepsilon = 0.5, 0.55$ and 0.6 (5% case) for obtaining the interference signal. Recall that as ε increases as the reliability of estimating the interference signal improves.

For instance, Fig.10 shows the importance of updating node C's knowledge regarding the interference signal from node A. Clearly, this figure shows the BER when node C does not update its information as well as updates its information every 5% and 25%, respectively. Furthermore, it also shows that updating every 5% has lower BER than the other two cases. Note however that more frequent updating requires more computational complexity at node C.

Remark-4: Comparing the results obtained for half- and full-duplex transmission show that the performance of the full-duplex mode is slightly better than the performance of the half-duplex mode. These results show that the throughput for full-duplex is higher than that of the half-duplex case but at the cost of increased complexity at both the transmitter and receiver.

Remark-5: A trade-off between using either one codeword as shown before or a combination of two different codewords at node C can be easily drawn. In particular, in this case, the cognitive transmitter can use two different codewords for transmission. For example, the data are divided into two parts. Namely, the first part is encoded using a low rate code. Then, after updating the cognitive transmitter's estimate regarding the interference signal, the second part is encoded with a higher rate code. Even thought more information can be sent using a combination of two codewords the system BER is increased.

V. Conclusion

In this paper, a causal-DPC scheme in which the secondary transmitter can sense the environment and cognitively obtain the interference signal has been presented. A two phase transmission scheme to estimate the interference signal and then employ DPC at the cognitive transmitter has been described. Moreover, the amount of data that the cognitive transmitter needs to listen and then start transmission has been lower bounded. Performance results have been shown for both causal half-duplex and full-duplex transmission and also compared with a non-causal system. Furthermore, these results are valid for arbitrary interference power. Future research could concentrate on improving the performance of the practical DPC code using other codes and receiver structures that use a combination of interference cancellation at the receiver with decoding of DPC codes.

Acknowledgments

The authors would like to thank the anonymous reviewers for their helpful and constructive comments in both the technical content and the presentation of this work.

Appendix A
Computation of the Power Inflation Factor

In this appendix, we derive the optimal power inflation factor β. We initially transform the channel over the cognitive link into its equivalent modulo lattice additive noise (MLAN) channel [20], [21]. Specifically, this MLAN channel contains only the transmitted quantized vector q corrupted by the equivalent additive noise seen by the receiver $z^{'}$. The received signal in (8) is first multiplied by h^*_{CD} to compensate for the phase of the signal. After that, this signal is multiplied by the power inflation factor β and then the result is fed to the non-linear modulo operation as shown in Fig. 3(b). Thus, the signal to be decoded is given as

$$y^{'}_{D} = [\beta h^*_{CD} y_D] mod \Lambda \tag{12}$$

Now, we substitute the value of y_D from (8) in (12), so that the modified received signal is

$$y_D^{'} = [\beta|h_{CD}|^2 x_C + \beta h_{CD}^* h_{AD} x_A + \beta h_{CD}^* z_D] \, mod \, \Lambda \quad (13)$$

In this scenario, all the channel state information are assumed to be available at the transmitter [29], [16]. Therefore, the auxiliary random variable which was proposed by Costa [3] $q = x + \beta s$ has to be modified to consider these channel gains. Let us assume that the modified auxiliary random variable is given as

$$q = x_C + \ \xi \beta y_C \quad (14)$$

where ξ is a factor related to the availability of the channel state information at the transmitter and has to be determined. Now, we plug the value of x_C from (14) in (13) to compute the value of ξ that ensures the received signal in (13) is interference free. Thus, the formula in (15) is obtained.

In order to get the value of ξ, the sum of the coefficients of x_A should be 0. Therefore, $\xi = h_{AD}/(|h_{CD}|^2 h_{CD})$ is obtained. Subsequently, the values of ξ and y_C are plugged in (14) and after some algebraic manipulations, thus,

$$\beta h_{CD}^* h_{AD} x_A = |h_{CD}|^2 q - |h_{CD}|^2 x_C - \beta \frac{h_{CD}^* h_{AD}}{h_{AC}} z_C \quad (16)$$

We then substitute the value of $\beta h_{CD}^* h_{AD} x_A$ from (16) into (13) and also employ the modulo lattice distributive property [33]

$$[(x \, mod \, \Lambda) + y] = [x + y] \, mod \, \Lambda \quad (17)$$

such that (13) can be re-written as shown in (18), where $z^{'}$ as given in (19) is the equivalent noise seen by the receiver. Hence, the equivalent noise contains noise due to quantization at both the transmitter and receiver, and Gaussian noise added by the channels from the primary transmitter to the secondary transmitter z_C and that from the cognitive transmitter to its destination, z_D.

The transmitted symbols x_C and the noise signals z_C and z_D are assumed to be independent with variance P_C , P_{z_C} and P_{z_D} respectively. Thus, the variance of the equivalent noise is computed as in (20). Finally, we minimize the equivalent noise power in (20) over all values of β. Thus, for fixed values of P_C , P_{z_C} and P_{z_D}, we set the derivative of $P_{z'}$ with respect to β equal to 0 to obtain the power inflation factor in (9).

References

[1] S.Gelfand and M.Pinsker, "Coding for channel with random parameters," in *Problems of Control and Information Theory*, 1980.

[2] G. Caire and S. Shamai, "On the capacity of some channels with channel state information," *IEEE Trans. Inf. Theory*, vol. 45, no. 6, pp. 2007–2019, Sept. 1999.

[3] M. Costa, "Writing on dirty paper (corresp.)," *IEEE Trans. Inf. Theory*, vol. 29, no. 3, pp. 439–441, May. 1983.

[4] H. Bagheri, A. Motahari, and A. Khandani, "Zero-forcing for the symmetric interference channel with conferencing encoders," in *Proc. 2010 IEEE Int. Symp. Inf. Theory*, pp. 370–374.

[5] I.-H. Wang and D. Tse, "Interference mitigation through limited transmitter cooperation," *IEEE Trans. Inf. Theory*, vol. 57, no. 5, pp. 2941–2965, 2011.

[6] G. Caire and S. Shamai, "On the achievable throughput of a multi-antenna Gaussian broadcast channel," *IEEE Trans. Inf. Theory*, vol. 49, no. 7, pp. 1691–1706, 2003.

[7] S. Gaur, J. Acharya, and L. Gao, "Enhancing ZF-DPC performance with receiver processing," *IEEE Trans. Wireless Commun.*, vol. 10, no. 12, pp. 4052–4056, 2011.

[8] L.-N. Tran, M. Juntti, M. Bengtsson, and B. Ottersten, "Beamformer designs for MISO broadcast channels with zero-forcing dirty paper coding," *IEEE Trans. Wireless Commun.*, vol. 12, no. 3, pp. 1173–1185, 2013.

[9] W. Wu, S. Vishwanath, and A. Arapostathis, "Capacity of a class of cognitive radio channels: interference channels with degraded message sets," *IEEE Trans. Inf. Theory*, vol. 53, no. 11, pp. 4391–4399, 2007.

[10] S. Rini, D. Tuninetti, and N. Devroye, "The capacity region of Gaussian cognitive radio channels to within 1.81 bits," in *Proc. 2010 IEEE Inf. Theory Workshop*, pp. 1–5.

[11] I.-H. Wang and D. Tse, "Interference mitigation through limited transmitter cooperation," in *Proc. 2010 IEEE Int. Symp. Inf. Theory*, pp. 380–384.

[12] V. Prabhakaran and P. Viswanath, "Interference channels with source cooperation," *IEEE Trans. Inf. Theory*, vol. 57, no. 1, pp. 156–186, 2011.

[13] Y. Peng and D. Rajan, "Achievable rate of Gaussian cognitive Z-interference channel with partial side information," in *2009 IEEE Global Telecommun. Conf.*

[14] M. Mazzotti and M. Chiani, "A simple rate-1/2 co-decoding scheme for writing on dirty paper," in *Proc. 2006 IEEE Int. Conf. Commun.*, pp. 1622–1627.

[15] G. Kyung and C. Wang, "On the designs and challenges of practical binary dirty paper coding," in *2009 IEEE Global Telecommun. Conf.*

[16] S.-C. Lin and H.-J. Su, "Practical vector dirty paper coding for MIMO Gaussian broadcast channels," *IEEE J. Sel. Areas Commun.*, vol. 25, no. 7, pp. 1345–1357, Sept. 2007.

[17] P. Lin, S. Lin, C. Lee, and H. Su, "Cognitive radio with partial channel state information at the transmitter," *IEEE Trans. Wireless Commun.*, vol. 9, no. 11, pp. 3402–3413, Nov. 2010.

[18] U. Erez and S. Brink, "A close-to-capacity dirty paper coding scheme," *IEEE Trans. Inf. Theory*, vol. 51, no. 10, pp. 3417–3432, Oct. 2005.

[19] G. Shilpa, A. Thangaraj, and S. Bhashyam, "Dirty paper coding using sign-bit shaping and LDPC codes," in *Proc. 2010 IEEE Int. Symp. Inf. Theory*, pp. 923–927.

[20] U. Erez, S. Shamai, and R. Zamir, "Capacity and lattice strategies for cancelling known interference," *IEEE Trans. Inf. Theory*, vol. 51, pp. 3820–3833, 2005.

[21] U. Erez and R. Zamir, "Achieving 1/2 log (1+SNR) on the AWGN Channel with lattice encoding and decoding," *IEEE Trans. Inf. Theory*, vol. 50, no. 10, pp. 2293–2314, Oct. 2004.

[22] R. Fischer, W. Marcellin, and M. Wang, "Trellis-coded vector quantization," *IEEE Trans. Inf. Theory*, vol. 37, pp. 1551–1566, 1991.

[23] H. Wang and N. Moayeri, "Trellis coded vector quantization," *IEEE Trans. Commun.*, vol. 40, pp. 1273–1276, 1992.

[24] E. Aydin and I. Altunbas, "Serially concatenated LDPC and space-time trellis codes with transmit antenna selection," in *IEEE Signal Process. Commun. Applications*, Apr. 2006, pp. 1–4.

[25] W. Ryan, *Concatenated Convlutional Codes and Iterative Decoding*. John Wiley & Sons, 2003, Wiley Encyclopedia of Telecommunications.

[26] B.Vucetic and J.Yuan, *Space-Time Coding*. John Wiley & Sons, 2003.

[27] A. del Coso Sanchez, "Achievable rates for Gaussian channels with multiple relays," Ph.D. dissertation, Universitat Polit'ecnica de Catalunya, 2008.

[28] G. Kramer, A. Ashikhmin, A. van Wijngaarden, and X. Wei, "Spectral efficiency of coded phase-shift keying for fiber-optic communication," *J. Lightwave Technol.*, vol. 21, no. 10, pp. 2438–2445, Oct. 2003.

[29] A. Jovicic and P. Viswanath, "Cognitive radio: an information-theoretic perspective," *IEEE Trans. Inf. Theory*, vol. 55, no. 9, pp. 3945–3958, Sept. 2009.

[30] P. Frenger, P. Orten, and T. Ottosson, "Convolutional codes with optimum distance spectrum," *IEEE Commun. Lett.*, vol. 3, no. 11, pp. 317–319, Nov. 1999.

[31] Z. Al-qudah and D. Rajan, "Multiple input multiple output dirty paper coding: system design and performance," in *2012 Int. Conf. Comput., Netw. Commun.*

[32] E. Page, "Binary decoding of concatenated turbo codes and space-time block codes for quaternary modulations," in *Proc. 2004 IEEE Mediterranean Electrotechnical Conf.*, vol. 3, pp. 1159–1164.

[33] Richard.Blahut, *Theory and Practice of Error Control Codes*. Addison-Wesley, 1983.

$$y_D^{'} = [\beta|h_{CD}|^2 \left(q - \beta\xi|h_{AC}|^2 x_A - \beta\xi h_{AC}^* z_C\right) + \beta h_{CD}^* h_{AD} x_A + \beta h_{CD}^* z_D] \, mod\, \Lambda \tag{15}$$

$$\begin{aligned} y_D^{'} &= [\beta|h_{CD}|^2 x_C + (\beta h_{CD}^* h_{AD} x_A) \, mod\, \Lambda + \beta h_{CD}^* z_D] \, mod\, \Lambda \\ &= [\beta|h_{CD}|^2 x_C + (|h_{CD}|^2 q - |h_{CD}|^2 x_C - \beta \frac{h_{CD}^* h_{AD}}{h_{AC}} z_C) \, mod\, \Lambda + \beta h_{CD}^* z_D] \, mod\, \Lambda \\ &= [|h_{CD}|^2 q - |h_{CD}|^2 x_C (1-\beta) - \beta \frac{h_{CD}^* h_{AD}}{h_{AC}} z_C + \beta h_{CD}^* z_D] \, mod\, \Lambda \\ &= [q + z^{'}] \, mod\, \Lambda \end{aligned} \tag{18}$$

$$z^{'} = \frac{1}{|h_{CD}|^2} \left(-|h_{CD}|^2 x_C (1-\beta) - \beta \frac{h_{CD}^* h_{AD}}{h_{AC}} z_C + \beta h_{CD}^* z_D\right) \tag{19}$$

$$P_{z^{'}} = \frac{1}{|h_{CD}|^4} \left(|h_{CD}|^4 P_C (1-\beta)^2 + \beta^2 \frac{|h_{CD}|^2 |h_{AD}|^2}{|h_{AC}|^2} P_{z_C} + \beta^2 |h_{CD}|^2 P_{z_D}\right) \tag{20}$$

Zouhair Al-Qudah received the B.Sc. in Telecommunication Engineering from Yarmouk University, Jordan in 2002, the M.Sc. in Electrical Engineering, with emphasis on digital communications and signal processing for wireless communication, from Kalmar University College, Sweden in 2006, and the Ph.D. degree in Electrical Engineering from Southern Methodist University at Dallas, Texas in 2013. From September 2002 and August 2004, he served as a technical and service engineer at Communication directorate of the public security department at Amman, Jordan. From March 2007 and August 2009, he worked as a full time lecturer at Yanbu College of Technology, Saudi Arabia. Since September 2013, he has been with Al-Hussein Bin Talal university at Ma'an, Jordan, where he is currently an Assistant Professor. His research interest span various aspects of multipath fading channels, including Multiuser information theory, interference cancellation techniques, and practical coding techniques for Dirty Paper problem.

Dinesh Rajan received his B.Tech degree from Indian Institute of Technology (IIT), Madras in Electrical Engineering. He was also awarded the M.S and Ph.D degrees from Rice University, Houston, Texas both in the areas of Electrical and Computer Engineering. He is currently Department Chair and Professor in the Electrical Engineering Department at Southern Methodist University (SMU), Dallas, Texas. His current research interests include communications theory, wireless networks, information theory and computational imaging. He received a National Science Foundation CAREER award in 2006 for his work on applying information theory to the design of mobile wireless networks.